Neurocomputing 74 (2011) 1026–1034

Contents lists available at ScienceDirect

Neurocomputing

journal homepage: www.elsevier.com/locate/neucom

Interactions between two neural populations: A mechanism of chaos and oscillation in neural mass model

Gan Huang *, Dingguo Zhang, Jiangjun Meng, Xiangyang Zhu

State Key Laboratory of Mechanical System and Vibration, Shanghai Jiao Tong University, Shanghai 200240, China

ARTICLE INFO

Article history:
Received 12 July 2010
Received in revised form
18 November 2010
Accepted 27 November 2010
Communicated by Z. Wang
Available online 17 December 2010

Keywords:
Neural mass model
Chaos
Oscillation
EEG
Epilepsy

ABSTRACT

Neural mass model developed by Lopes da Silva et al. is able to describe limit cycle behavior in Electroencephalography (EEG) of alpha rhythm and exhibit complex dynamics between cortical areas. In this work, we extend Grimbert and Faugeras's work to study the dynamical behavior caused by interaction of cortical areas. The model is developed with the coupling of two neural populations. We show that various attractors, including equilibrium points, periodic solutions and chaotic strange attractors, could coexist in different ways with different value of the connectivity parameters. The main findings are that: (1) The stable equilibrium points only appear with a small value of the parameter. (2) While the alpha activities always exist for both two populations with proper initial conditions. Interestingly, the coexistence of the multiple alpha-to-epileptic activities implies the multiple coupling ways for these activities in phase. Two neuronal populations with epileptic activities could interact with multiple rhythms depending on their connectivity. (3) For particular interest, chaotic behaviors are identified in four regions divided by the connectivity parameter with the positive maximal Lyapunov exponent. The four types of chaotic attractors have their own structures, but all of them are related to the epileptic activities.

1. Introduction

Electroencephalography (EEG) is the recording of electrical brain activity on the scalp. It reflects correlated synaptic activity caused by post-synaptic potentials of cortical neurons. The EEG is typically described as rhythmic activity, which can be decomposed into distinct bands by frequency (delta: up to 4 Hz, theta: 4–7 Hz, alpha: 8–12 Hz, Beta: 12–30 Hz, Gamma: 30–100 Hz). In neurology, the main diagnostic application of EEG is in the case of epilepsy, as epileptic activity can create clear abnormalities on a standard EEG study. To simulate the electrical brain activity and its intricate cortical structures, various mathematical models have been developed [5]. Wilson and Cowan [25] showed that a set of coupled nonlinear differential equations exhibits hysteresis phenomena and rhythmic activity. They suggested that the limit cycle oscillations generated by this model may mimic the EEG rhythm, and a conclusion supported it subsequently by Freeman [7]. In 1970s,Lopes Da Silva et al. developed a lumped parameter model to simulate the alpha rhythm [16,15,8]. The lumped parameter model makes it possible to reduce the complex dynamic system comprising a very large number of neurons into relatively simple circuits. Jansen's neural mass model [12], extended from the lumped parameter models of Lopes Da Silva, generates EEG signals from inhibitory and excitatory interactions within and between populations of neurons. The frequency of oscillations is determined by the kinetics of the population dynamics.

The neural mass model can also be used to learn the spatial distribution of the brain activities. Jansen et al. coupled two neural mass to reproduce the alpha and beta oscillations typically found in the visual cortex and the prefrontal cortex. The interactions between two populations are described by linear transformations with proper delays and interconnected constants. David and Friston found coupling can induce phase-lock activity [4]. They also compared four linear and nonlinear measures in detecting the functional connectivity among cortical areas [3]. The epileptic activity is traditionally assumed to be a collective behavior of neuronal synchronization at the cellular level. An epileptogenic network composed of three units were developed by Wendling et al. [23]. They tried to determine the causality relations among signals from this network.

Chaos and brain are really two giants in terms of complexity [2]. EEG signals have been considered to result either from random processes or to be generated by non-linear dynamic systems exhibiting chaotic behavior. In the past decades, numerous efforts have been directed towards ascertaining chaos in cortical signals [9,20, 19,17,1]. A review for chaos in brain can be seen in Ref. [13]. In the neural mass model, the pulse density $p(t)$ represents the excitatory input from neighboring or more distant areas. Jansen and Rit [12] chose the input $p(t)$ to be the random white noise ranging from 120 to 320 pulses per second. The increasing parameter C results in an output evolving from disorder to order and finally becomes disorder again (Fig. 2).

* Corresponding author.
E-mail address: huanggan1982@gmail.com (G. Huang).

0925-2312/$ - see front matter © 2010 Elsevier B.V. All rights reserved.
doi:10.1016/j.neucom.2010.11.019

Mathematically, Grimbert and Faugeras investigated the dynamical behavior of the neural mass model as a function of its input [11]. In their analysis, the rhythmic activities of alpha rhythm and epileptic wave are related to the structure of a set of periodic orbits and their bifurcation. However, the analysis is limited in single neural population. In this work, we extend Grimbert and Faugeras's work to the coupled neural mass model. The excitatory input is kept constant and two neural populations are connected with the connection strength as a parameter. As Grimbert and Faugeras said, "this is a difficult task". The emerging properties and the linearly increased system dimension make it more difficult to do mathematical analysis. As an alternative, numerical simulation is used to investigate population responses with various initial values. Attentions are paid to the emergence and the possible chaotic behaviors in the interactions. In Ref. [11], Grimbert and Faugeras treated the single population model as a deterministic system with p keeping constant. No chaotic attractor has been reported in the single population.

The remainder of this paper is organized as follows. Section 2 provides a brief description of neural mass model, and the behaviors of single population are introduced with random and constant inputs. Section 3 presents the simulation results for the coupled neural mass model. The results are discussed in Section 4, and the conclusion is given in Section 5.

2. Model description

2.1. Single population model

In Jansen's model, each of the neural populations involves two operators. The first one transforms the average pulse density of action potentials into an average postsynaptic membrane potential with the response function given by

$$h_e(t)=\begin{cases} Aate^{-at} & \text{if } t\geq 0 \\ 0 & \text{else} \end{cases}$$

for excitatory case and

$$h_i(t)=\begin{cases} Bbte^{-bt} & \text{if } t\geq 0 \\ 0 & \text{else} \end{cases}$$

for inhibitory case, where A and B determines the maximal amplitude of the excitatory and inhibitory post-synaptic potentials, respectively, and a and b lumps the characteristic delays of the synaptic transmission together. This operator can also be described as a set of linear second-order ordinary differential equations,

$$\ddot{y}=Aax-2a\dot{y}-a^2y$$

$$\ddot{y}=Bbx-2b\dot{y}-b^2y$$

where x, y are the input and output signals, which can also be written as follows:

$$\begin{cases} \dot{y}=z \\ \dot{z}=Aax-2az-a^2y \end{cases}$$

$$\begin{cases} \dot{y}=z \\ \dot{z}=Bbx-2bz-b^2y \end{cases}$$

The second operator transforms the average membrane potential of a population into an average pulsed density of action potentials fired by the neurons, which is represented by a non-linear sigmoid function

$$\mathrm{Sigm}(v)=\frac{2e_0}{1+e^{r(v_0-v)}}$$

where e_0, r, and v_0 are parameters to determine its shape.

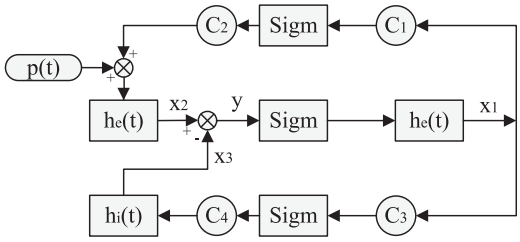

Fig. 1. Neural mass model with single neural population.

As described in Fig. 1, a single neural population is modelled by a population of pyramidal cells, receiving inhibitory and excitatory feedback from local neurons and excitatory input from far and near cortex areas with the connectivity constant $C_1,\ldots,C_4$. The following set of six differential equations can be used to describe the model:

$$\begin{cases} \dot{x}_1=x_4 \\ \dot{x}_2=x_5 \\ \dot{x}_3=x_6 \\ \dot{x}_4=Aa\ \mathrm{Sigm}(x_2-x_3)-2ax_4-a^2x_1 \\ \dot{x}_5=AaC_2\ \mathrm{Sigm}(C_1x_1)-2ax_5-a^2x_2+Aap \\ \dot{x}_6=BbC_4\ \mathrm{Sigm}(C_3x_1)-2bx_6-b^2x_3 \end{cases} \tag{1}$$

where $y=x_2-x_3$ is the output of the system.

The standard value of the parameters is determined anatomically as

$$A=3.25\ \text{mV},\quad a=100\ \text{s}^{-1}$$

$$B=22\ \text{mV},\quad b=50\ \text{s}^{-1}$$

$$e_0=2.5\ \text{s}^{-1},\quad r=0.56\ \text{mV}^{-1},\quad v_0=6\ \text{mV}$$

$$C_1=1.25C_2=4C_3=4C_4=C=135$$

The excitatory input is represented by an average pulse density $p(t)$, which can be random or deterministic. Jansen and Rit chose $p(t)$ to be a uniformly distributed random noise between 120 and 320 [12]. The alpha-like activity would be achieved for $C=135$ as shown in Fig. 2.

Grimbert and Faugeras [11] treated the input p as a constant, and analyzed the dynamic behaviors of Jansen's model as a function of p. Let $X=(x_1,x_2,x_3,x_4,x_5,x_6)^T$, and system (1) can be written as

$$\dot{X}=f(X,p)$$

The fixed points will be obtained by solving the equations $f(X,p)=0$, which leads to the implicit equation

$$y=\frac{A}{a}\left[C_2\mathrm{Sigm}\left(C_1\frac{A}{a}\mathrm{Sigm}(y)\right)+p\right]-\frac{B}{b}C_4\mathrm{Sigm}\left(C_3\frac{A}{a}\mathrm{Sigm}(y)\right)$$

where $y=x_2-x_3$ can be thought of as a function of parameter p.

The dynamic behaviors are sketched in Fig. 3, where x_1, x_2 and x_3 are the average post membrane potential of the corresponding neurons. For $p=50$, two equilibrium points coexist for system (1). As p increases to 110, the equilibrium point on the upper branch turns to be alpha-like limit cycle. When p grows to 130, the equilibrium point on the lower branch becomes spike-like epileptic limit cycle.

2.2. Coupled populations model

The single population model focus on the brain's dynamic behaviors of a separate area. While the spatial characters of the

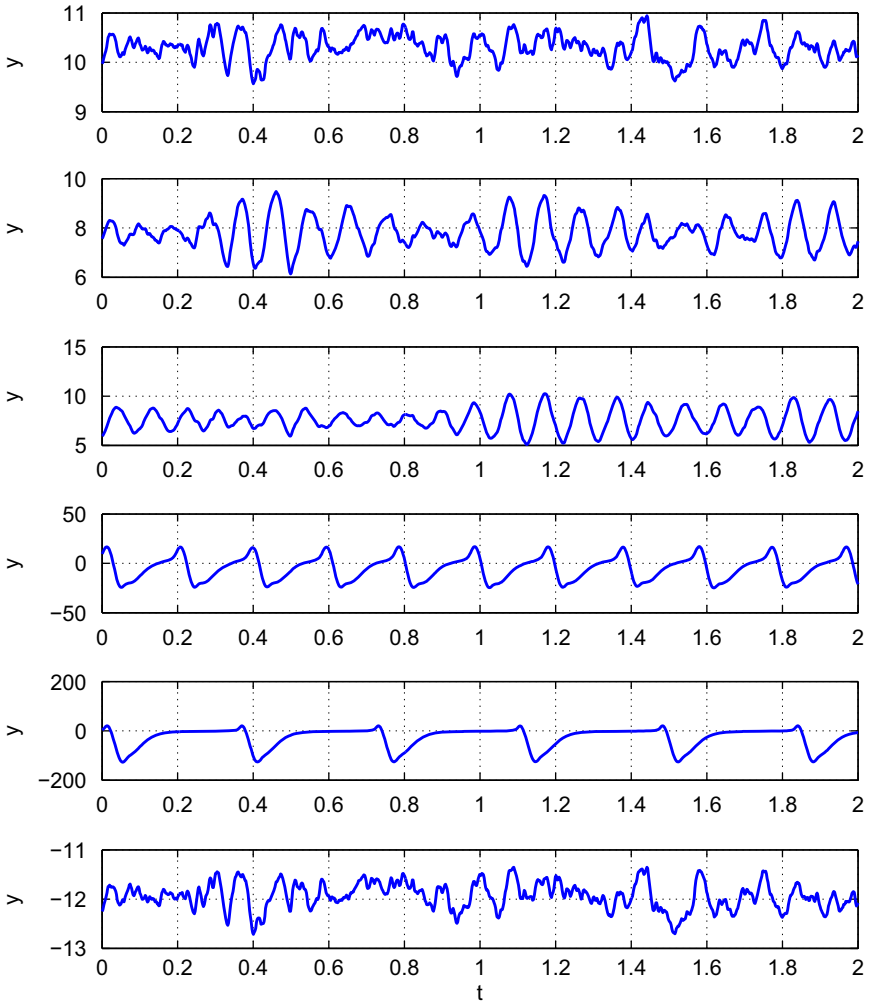

Fig. 2. The model's output $y=x_2-x_3$ with the lumped connectivity constant C equals (from top to bottom) 68, 128, 135, 270, 675, and 1350, respectively. The input is uniformly distributed random noise. The alpha-like activity has been obtained with $C=135$.

EEG signals cannot be simulated by the signal model. Jansen et al. used coupled model with two populations to explore the hypothesis that certain VEP components are due to the interaction between two or more cortical areas. Fig. 4 describes the schematic diagram of the coupled neural mass model. In their model, the two areas, which represented the visual cortex and the prefrontal cortex, were assumed to have the similar neuronal architecture. They share the same parameters (e.g. A, B and v_0). The input for each population comes from the external is represented by p_1 and p_2. Two connectivity constants, k_1 and k_2, attenuate the output of one area before it is fed to the other, and a_d is the delays. The two cortical areas are linked to each other via two other cortical areas: the extrastriate cortex and the inferotemporal cortex. Hence at least three neurons are necessary to account for the pathways of the processing of a visual stimulus by the prefrontal cortex and three more for feedback to the occipital visual cortex. The impulse response $h_d(t)$, similar to $h_e(t)$, can be used as

$$h_d(t)=\begin{cases} Aa_d t e^{-a_d t} & \text{if } t\geq 0 \\ 0 & \text{else} \end{cases}$$

where $a_d=a/3$ means a latency 3 times longer than the excitatory impulse response from local neurons. In Ref. [12], the authors set this parameters to simulate the connection between the prefrontal cortex and the occipital visual cortex. Hence, the two-neuron population model can be described as Eq. (2):

$$\begin{cases} \dot{x}_1 = x_4 \\ \dot{x}_2 = x_5 \\ \dot{x}_3 = x_6 \\ \dot{x}_4 = Aa\ \mathrm{Sigm}(x_2-x_3)-2ax_4-a^2x_1 \\ \dot{x}_5 = AaC_2\ \mathrm{Sigm}(C_1x_1)-2ax_5-a^2x_2 \\ \qquad +Aa(p_1+k_1x_{14}) \\ \dot{x}_6 = BbC_4\ \mathrm{Sigm}(C_3x_1)-2bx_6-b^2x_3 \\ \dot{x}_7 = x_{10} \\ \dot{x}_8 = x_{11} \\ \dot{x}_9 = x_{12} \\ \dot{x}_{10} = Aa\ \mathrm{Sigm}(x_8-x_9)-2ax_{10}-a^2x_7 \\ \dot{x}_{11} = AaC_2\ \mathrm{Sigm}(C_1x_7)-2ax_{11}-a^2x_8 \\ \qquad +Aa(p_2+k_2x_{13}) \\ \dot{x}_{12} = BbC_4\ \mathrm{Sigm}(C_3x_7)-2bx_{12}-b^2x_9 \\ \dot{x}_{13} = x_{15} \\ \dot{x}_{14} = x_{16} \\ \dot{x}_{15} = Aa_d\ \mathrm{Sigm}(x_2-x_3)-2a_dx_{15}-a_d^2x_{13} \\ \dot{x}_{16} = Aa_d\ \mathrm{Sigm}(x_8-x_9)-2a_dx_{16}-a_d^2x_{14} \end{cases} \quad (2)$$

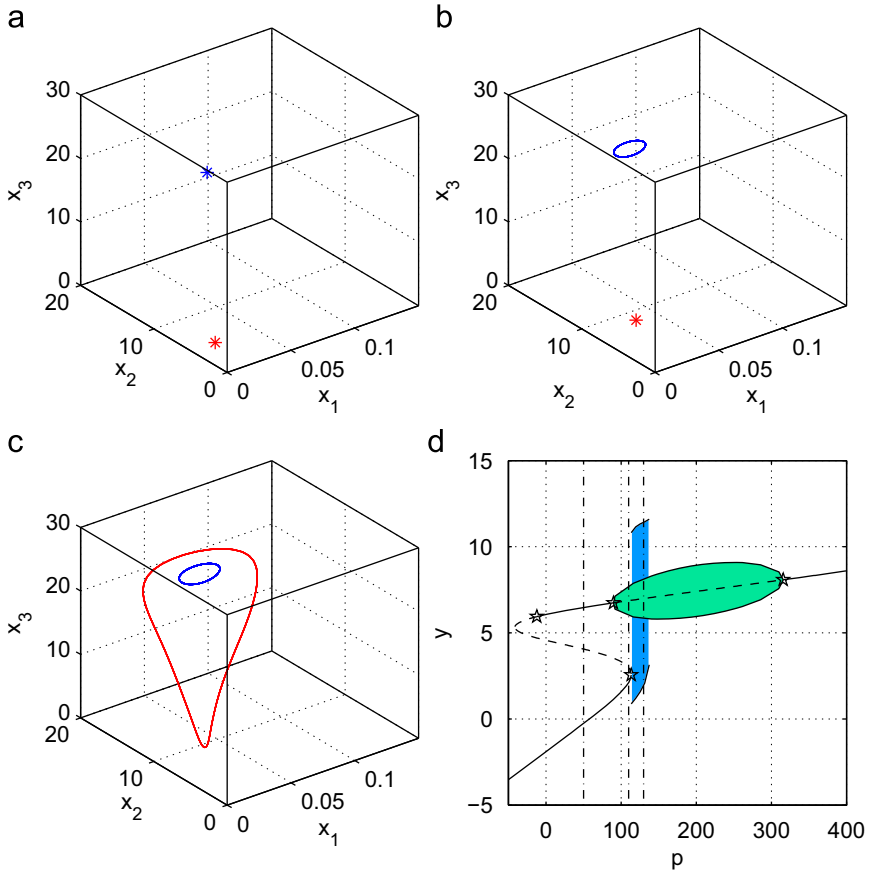

Fig. 3. (a) Two equilibrium points coexist for $p=50$ which is labelled by blue and red star respectively. (b) The alpha-like activity (blue cycle) and the equilibrium point (red star) coexist with the parameter $p=110$. (c) The alpha-like activity (blue cycle) and the spike-like epileptic activity (red cycle) coexist with the parameter $p=130$. (d) The bifurcation diagram for system (1). The stable fixed points (solid line) and the unstable fixed points (dashed line) are depicted with the critical points marked by pentagrams. The alpha-like limit cycles appear for each $p \in [89.83,315.70]$, and the spike-like epileptic limit cycles appear for each $p \in [113.58,137.38]$. The values of the parameter p, corresponding to subfigures (a)–(c), are represented with dashed-dotted lines on the diagram. (For interpretation of the references to color in this figure legend, the reader is referred to the web version of this article.)

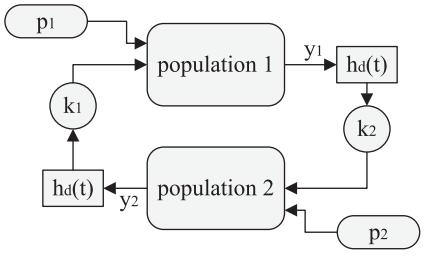

Fig. 4. Neural mass model with two neural populations connected.

Coupling two neural populations with the uncorrelated random input of p_1, p_2, Jansen et al. [12] studied the spatial distribution of alpha and beta activities, where k_1, k_2 vary between 0 and 120. Furthermore some evoked potentials were simulated by adding a transient component to the input of the coupled models.

Considering the inputs p_1 and p_2 as constants, the equilibrium points of system (2) can be obtained from the equations

$$\begin{cases} y_1 = \frac{A}{a}\left[C_2\ \mathrm{Sigm}\left(C_1\frac{A}{a}\mathrm{Sigm}(y_1)\right)+p_1+k_1\frac{A}{a_d}\mathrm{Sigm}(y_2)\right] \\ \qquad -\frac{B}{b}C_4\ \mathrm{Sigm}\left(C_3\frac{A}{a}\mathrm{Sigm}(y_1)\right) \\ y_2 = \frac{A}{a}\left[C_2\ \mathrm{Sigm}\left(C_1\frac{A}{a}\mathrm{Sigm}(y_2)\right)+p_2+k_2\frac{A}{a_d}\mathrm{Sigm}(y_1)\right] \\ \qquad -\frac{B}{b}C_4\ \mathrm{Sigm}\left(C_3\frac{A}{a}\mathrm{Sigm}(y_2)\right) \end{cases} \quad (3)$$

with the parameters p_1, p_2, k_1 and k_2. The singular point (y_1,y_2) of Eq. (3) leads to the corresponding singular point of system (2)

$$S(y_1,y_2) = [(A/a)\ \mathrm{Sigm}(y_1),(A/a)(C_2\ \mathrm{Sigm}(C_1(A/a)\ \mathrm{Sigm}(y_1))+p_1+k_1 (A/a_d)\ \mathrm{Sigm}(y_2)),(B/b)C_4\ \mathrm{Sigm}(C_3(A/a)\ \mathrm{Sigm}(y_1)),0,0,0,(A/a)\ \mathrm{Sigm}(y_2), (A/a)(C_2\ \mathrm{Sigm}(C_1(A/a)\mathrm{Sigm}(y_2))+p_2+k_2(A/a_d)\ \mathrm{Sigm}(y_1)),(B/b) C_4\mathrm{Sigm}(C_3(A/a)\ \mathrm{Sigm}(y_2)),\ 0,\ 0,\ 0,\ (A/a_d)\ \mathrm{Sigm}(y_1),(A/a_d)\ \mathrm{Sigm}(y_2),0,0]$$

The stability of the equilibrium point is determined by the Jacobian matrix of system (2). The Jacobian matrix with all eigenvalues negative indicates the equilibrium point $S(y_1,y_2)$ is stable.

3. Simulations and results

In this model, the inputs of the populations are configured with four parameters p_1, p_2, k_1 and k_2. The dynamics of single population with the input p is studied in Ref. [11]. Fig. 3 shows the condition especially for $p=50$, 110, and 130. In this simulation, in order to exhibit the rich dynamical behavior of the coupled system (2) in a simple way, the parameters are set as $p_1=110$, $p_2=50$, $k_1=K$ and $k_2=650-K$, where each K varies from 0 to 650. A one-dimensional study of the model parameter-space is conducted. The system is integrated for 40 s with 100 random initial conditions of K varied between 0 and 650 in step of 0.1. The fourth order Runge–Kutta method is used to solve the system of ordinary differential equation (2) with its maximal Lyapunov exponent (MLE) in Matlab.

The Lyapunov exponent describes the time asymptotic rate of separation of infinitesimally close trajectories. A positive MLE is

usually taken as an indication that the system is chaotic. MLE of zero indicates that a limit cycle exists in the system, and a stable fixed point has all Lyapunov exponents negative. More detailed discussions about the Lyapunov exponent and their relation to chaos can be seen from Refs. [6,18,24]. For system (2), the maximal Lyapunov exponent is calculated by taking three typical initial values

$$X_1 = \begin{bmatrix} 0.0400 & 14.1098 & 11.0059 & -0.4585 \\ -216.0680 & -189.0192 & 0.1104 & 23.8555 \\ 16.2095 & 0.1089 & -36.0743 & 36.5895 \\ 0.2075 & 0.3342 & -2.2957 & 0.5543 \end{bmatrix},$$

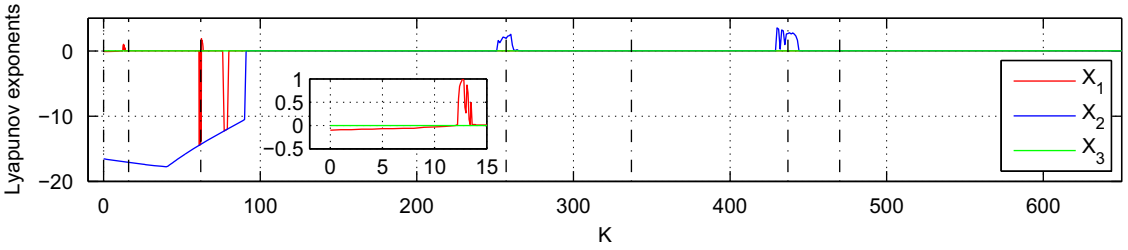

Fig. 5. The maximal Lyapunov exponent (MLE) of system (2) with parameters $K \in [0,650]$. The subfigure is the partial enlarged view for $K \in [0,15]$. The dashed-dotted line for $K=0,16,62,257,337,437,470$ indicates the positions for phase diagram plotted in Fig. 6. The line in red, blue and green is corresponding to the initial value X_1, X_2, X_3 respectively. The MLE is positive in four regions of $K \in [12.3,13.5]$, $[62.5,63.5]$, $[252,261]$ and $[431,444]$. For the initial value of X_1 (red), the MLE is negative for $K \in [0,12.2]$, and the negative and zero MLEs appear alternatively near the second region $K \in [62.5,63.5]$. For the initial value of X_2 (blue), the MLE is negative for $K \in [0,90]$. The zero MLE holds for all values of $K \in [0,650]$ with the initial value of X_3 (green). (For interpretation of the references to color in this figure legend, the reader is referred to the web version of this article.)

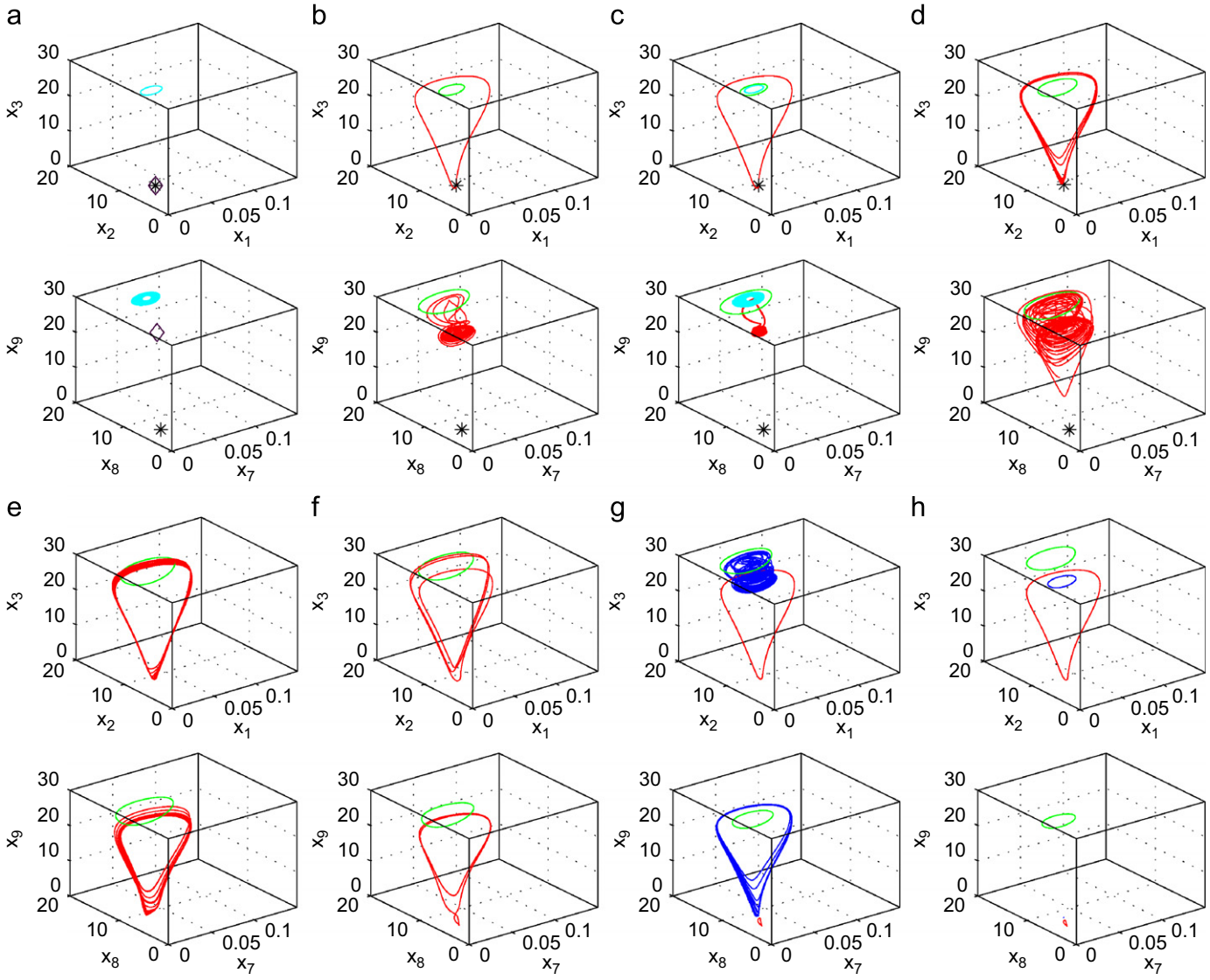

Fig. 6. The dynamic behavior of system (2) for parameters $K=0,12.7,16,62,257,337,433,470$. x_1, x_2 and x_3 are the average post membrane potentials of the corresponding neurons for population 1, and x_7, x_8 and x_9 correspond to population 2.

$$X_2 = \begin{bmatrix} 0.1477 & 21.6848 & 12.0221 & 0.4096 \\ 62.1496 & 349.1564 & 0.0300 & 11.4769 \\ 8.5745 & -0.3617 & -131.9716 & -133.8066 \\ 0.2590 & 0.1762 & 4.1132 & -2.0146 \end{bmatrix},$$

$$X_3 = \begin{bmatrix} 0.1011 & 20.5966 & 12.8552 & 0.8736 \\ 11.0675 & -12.2445 & 0.0828 & 25.1161 \\ 19.0421 & -0.7560 & -31.1860 & -146.1025 \\ 0.2891 & 0.3340 & 0.4683 & -1.8299 \end{bmatrix},$$

with red, blue and green in Fig. 5 respectively. Numerical experiments showed that this period of time 500 s was sufficiently long for the system to converge to a stable estimate of MLE.

Some dynamical behaviors are shown in Fig. 6 with the parameters K=0,12.7,16,62,257,337,433,470. All attractors are from time series of 5 s long, following the removal of an initial transient of 15 s.

3.1. Equilibrium points

Two stable equilibrium points exist in system (2). As shown in Fig. 6, one equilibrium point, marked by diamond, exists for $K \in [0, 12.2]$, and the other one, marked by star, exists for $K \in [0,140.2]$. In Fig. 5, we see that the MLE in red with the initial value X_1 for $K \in [0,12.2]$ is negative but close to zero. The more negative MLE in blue for $K \in [0,90]$ indicates the more stable equilibrium point with the initial value X_2. For $K \in [140.2,650]$, no equilibrium point exists any more.

3.2. Limit cycles

For the single population (1), the limit cycles corresponding to the alpha-like and spike-like epileptic activities are displayed in Fig. 3. Coupling two identical populations, the combinations of these activities are found in system (2), such as alpha-to-alpha, alpha-to-epileptic and epileptic-to-epileptic activities.

As plotted in green in Fig. 5, the solution with the initial value X_3 converges to the alpha-to-alpha cycle for all value of K in [0,650] with the corresponding MLE remaining 0. Since there is no feedback or weak feedback from populations 2 to 1, the quasi-periodic alpha-to-alpha cycle often occurs with zero or small value of K. Figs. 6(a) and (c) illustrate quasi-periodic orbits in cyan with K=0 and 16. As the value of K increases, the alpha-to-alpha cycle would be periodic. Figs. 6(b)–(h) show such cases in green. Especially, the coexistence of periodic and quasi-periodic alpha-to-alpha cycles can be observed for K=16 in Fig. 6(c). If $K \in [346,352]$, the alpha-to-alpha cycles would be globally attracted, and no other attractors have been found in the simulation.

The interaction of alpha and epileptic activities is more complex. In most instances, there is only one mode for the combination of alpha and epileptic activities, as shown in Fig. 6(c) with the red trajectory. However, it is not always the case. Fig. 7 depicts an interesting phenomenon of the coexistence of three alpha-to-epileptic cycles when K=36. Besides the black equilibrium point and the green alpha-to-alpha cycle, three types of alpha-to-epileptic cycles in red, pink, and yellow, respectively, are observed. They share the similar spike-like epileptic activities in population 1, but the different

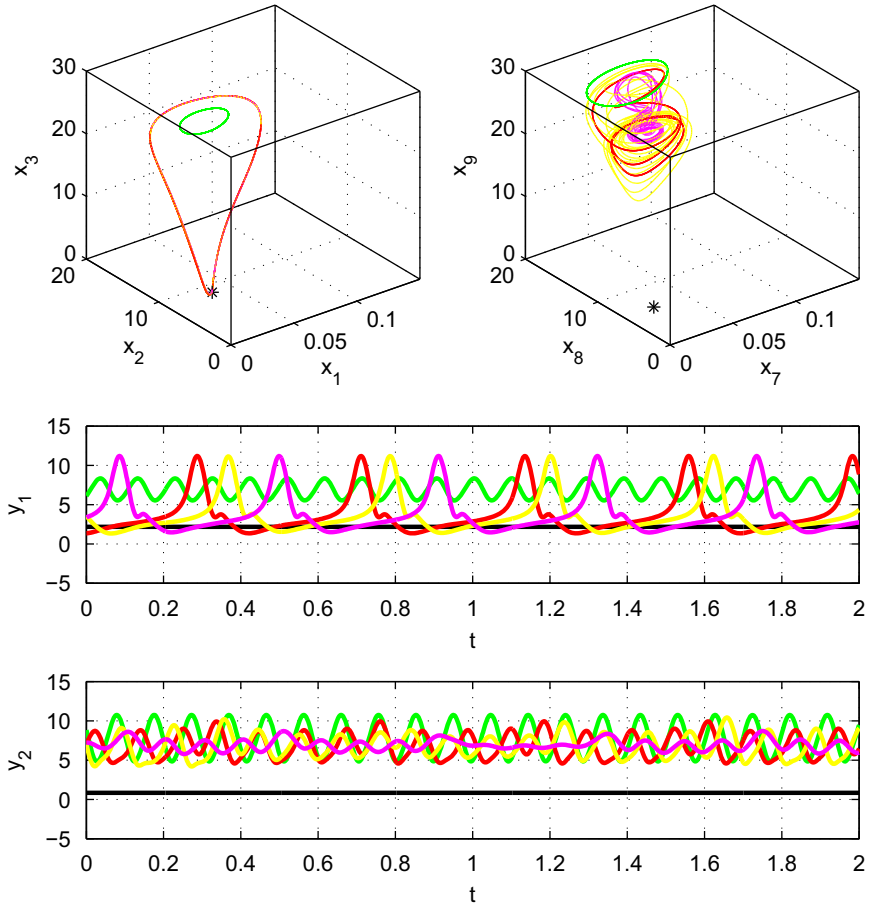

Fig. 7. The dynamic behavior of system (2) for parameter K=36. Besides the black equilibrium point and the green alpha-to-alpha cycle, there are three types of alpha-to-epileptic cycles shown in red, pink, and yellow respectively. (For interpretation of the references to color in this figure legend, the reader is referred to the web version of this article.)

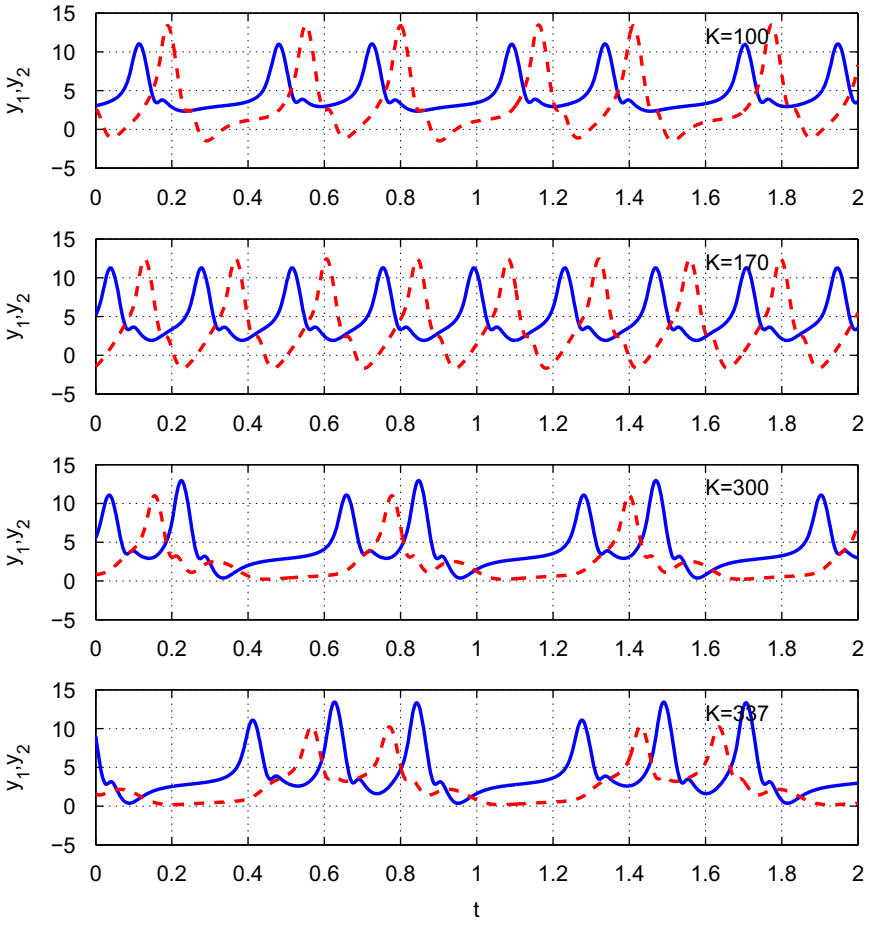

Fig. 8. The time response of y_1 (solid blue lines) and y_2 (dashed red line) with the parameter K equals (from top to bottom) 100, 170, 300, and 337, respectively. (For interpretation of the references to color in this figure legend, the reader is referred to the web version of this article.)

coupling modes in phase make the waveform of the alpha activities in population 2 differ greatly from each other.

Unlike multiple coupled modes of alpha-to-epileptic activities in different phases, the epileptic-to-epileptic activities can be coupled with different rhythms (Fig. 8). For $K=100$, two spikes of each population appear in one period. A spike for one period occurs with $K=170$. Further more, the coupled modes of two spikes vs. one spike, and three spikes vs. two spikes are shown in Fig. 8 with $K=300$ and 337, respectively. Fig. 6(f) depicts the phase diagram for the coupled mode of three spikes vs. two spikes in red.

The combination of equilibrium point and limit cycles is displayed in Fig. 6(h) for $K=470$. The combination of equilibrium point and alpha cycle is depicted in blue, and the coupling of equilibrium point and epileptic cycle is depicted in red.

3.3. Chaos

Besides limit cycles, the interaction of alpha and epileptic activities could also lead to chaotic behaviors for the coupled model (2). Four regions with the positive MLE are observed in Fig. 5, which indicates chaos in these regions. The alpha-to-epileptic chaotic attractors in regions $K \in [12.3,13.5]$, $K \in [62.5,63.5]$ and $K \in [431,444]$ are shown in Fig. 6 (b), (d) and (g), respectively. In region $K \in [252,261]$, a kind of epileptic-to-epileptic chaotic attractor is plotted in Fig. 6(e). As parameter K varies from 248 to 252, the system becomes chaotic undergoing a period-doubling process.

Remark. The positive MLE in the four regions, as shown in Fig. 5, does not mean the chaotic attractors only exist in these regions. The positive MLE in these regions indicates that the solutions with the corresponding initial values among x_1, x_2 and x_3 converge to chaotic attractors with the parameters K in these regions. The solutions with other initial values may converge to the chaotic attractors outside these regions. But no other special chaotic attractors are found in our simulations. Similarly, the MLE with the initial value x_2 is negative for $K \in [0,90]$, the blue line in Fig. 5. However, the corresponding equilibrium point, marked in black star in Figs. 6(a)–(d), exists in the region $K \in [0,142.2]$, which is determined by Eq. (3).

4. Discussion

In study of EEG activity, nonlinear measures such as correlation dimension, Lyapunov exponents, and nonlinear prediction error are often applied to time series with the intention of identifying the presence of nonlinearity, possibly chaotic behavior [19,17,1]. However, the presence of noise of unknown origin makes it hopeless to reinterpret the data within the frame of chaos theory. Theiler [20] reconsidered the epileptic EEG time series, which was previously reported to be chaotic, with the method of surrogate data. As a result, the correlation dimension, Lyapunov exponent estimator was essentially the same for the original and surrogate data sets. Freeman suggested the name of "stochastic chaos" to describe the unpredictability of brain oscillations, which manifests either limit cycle attractors, or chaotic attractors, or colored noise, or all of the above [10]. In study of neural mass model, the stochastic character is always considered with the excitatory input chosen to be a uniformly or Gaussian distributed noise [12,23,4,3]. The existence of noise makes the dynamic analysis of this model more difficult. Jansen et al. [12] roughly classified the

oscillatory behavior into several types with variations of the connectivity constants. The coexistence of multiple states could be observed in the noisy circumstance. In [11], Grimbert and Faugeras treated the model as a deterministic system with the input kept constant to study the underlying dynamics. A detailed stability and bifurcation analysis of the single neural mass model has been made as a function of its input.

In this work, the simulation study of the coupled neural mass model is an extension of dynamic analysis on single neuron population of Grimberty and Faugeras. The interaction of epileptic-to-epileptic and epileptic-to-alpha activities would also lead to some chaotic behaviors. No alpha-to-alpha activity is identified to be chaotic. It indicates that the chaotic behaviors in the EEG signals are correlated with epileptic behaviors, which is in accordance with Freeman's experiment [9]. In 1987, Freeman and his collaborators developed mathematical models for EEG signals generated by the olfactory system in rabbits. They suggested that epileptiform patterns extracted from EEG seizure signals can be explained through the chaotic dynamics of these models. In their model, the central olfactory system is made of three parts, the bulb, anterior nucleus, and prepyriform cortex. Each part can be seen as a mass of neurons. Here, chaotic behavior is generated with the interaction of two neuronal populations. By contrast, no chaotic behavior has been discovered in the single neuronal population or the direct coupled network, as $K=0$ or 650. Our study also shows the coexistence of chaotic behaviors and other stable attractors. Chaotic behavior in the four regions is accompanied by other activities, which means the system would also be non-chaotic with certain initial values.

5. Conclusions

The present study is performed on the coupled neural mass model with two neural populations. As the inputs p_1 and p_2 are kept constant, the noise-free system can help us to understand the deterministic nature of brain activity. For single population, the equilibrium points, alpha and epileptic periodic orbits can be observed with the varying of the excitatory input. In the interaction of two populations, the varying of parameter K leads to rich and varied dynamical behaviors of the system. Stable equilibrium points, periodic orbits, quasi-periodic orbits and chaos could be observed in the system. With the weak connection from populations 1 to 2, an alpha-to-alpha quasi-periodic orbit and two equilibrium points coexist in the system. As the parameter K increases, the equilibrium points disappear one by one, and the alpha-to-alpha activities turns to be periodic. The combination of the alpha activities is simple and ubiquitous. In contrast, the epilepsy is more complex in the interaction, and its activities do not exist in the entire region of $K \in [0, 650]$. There exist multiple ways for epileptic activities in the interaction with other activities. The epileptic activities can interact with alpha activities in different phases. Two epileptic activities could be coupled in different rhythms. Furthermore, chaotic behavior was identified with the measure of MLE in four regions of parameter space of K. All of them are related to epileptic activities. The coexistence of various attractors is a key feature of the system. The number of stable attractors could be only 1 for $K \in [346,352]$ where the alpha-to-alpha activity is the global attractor, or up to 5 as illustrated in Fig. 7 with $K=36$. Here, we limited the number of neuron populations to 2, complex dynamics under the changes of network structures deserve further investigation. Some stochastic differential methods [21,14,22] may help us to analysis the network with multiple neuron populations.

Acknowledgements

This work is supported by National High Technology Research and Development Program of China (no. 2009AA04Z212), Research Fund for the Doctoral Program of Higher Education of China (no. 20090073120047), and National Natural Science Foundation of China (no. 51075265).

References

[1] A. Celletti, A.E.P. Villa, Low-dimensional chaotic attractors in the rat brain, Biological Cybernetics 74 (5) (1996) 387–393.
[2] A. Das, 〈http://www.cerebromente.org.br/n14/mente/chaos.html〉.
[3] O. David, D. Cosmelli, K.J. Friston, Evaluation of different measures of functional connectivity using a neural mass model, NeuroImage 21 (2) (2004) 659–673.
[4] O. David, K.J. Friston, A neural mass model for MEG/EEG: coupling and neuronal dynamics, NeuroImage 20 (3) (2003) 1743–1755.
[5] G. Deco, V.K. Jirsa, P.A. Robinson, M. Breakspear, K. Friston, The dynamic brain: from spiking neurons to neural masses and cortical fields, PLoS Computational Biology 4 (8).
[6] J.P. Eckmann, D. Ruelle, Ergodic theory of chaos and strange attractors, Reviews of Modern Physics 57 (3) (1985) 617–656.
[7] W.J. Freeman, Mass Action in the Nervous System, Academic Press, New York, 1975.
[8] W.J. Freeman, Models of the dynamics of neural populations, Electroencephalography and Clinical Neurophysiology. Supplement, (34):9, 1978.
[9] W.J. Freeman, Simulation of chaotic EEG patterns with a dynamic model of the olfactory system, Biological Cybernetics 56 (2) (1987) 139–150.
[10] W.J. Freeman, A proposed name for aperiodic brain activity: stochastic chaos, Neural Networks 13 (1) (2000) 11–13.
[11] F. Grimbert, O. Faugeras, Bifurcation analysis of Jansen's neural mass model, Neural Computation 18 (12) (2006) 3052–3068.
[12] B.H. Jansen, V.G. Rit, Electroencephalogram and visual evoked potential generation in a mathematical model of coupled cortical columns, Biological Cybernetics 73 (4) (1995) 357–366.
[13] H. Korn, P. Faure, Is there chaos in the brain? II. Experimental evidence and related models, Comptes Rendus Biologies 326 (9) (2003) 787–840.
[14] J. Liang, Z. Wang, X. Liu, On passivity and passification of stochastic fuzzy systems with delays: the discrete-time case, IEEE Transactions on Systems, Man, and Cybernetics, Part B: Cybernetics 40 (3) (2010) 964–969.
[15] S.F.H. Lopes, A. Van Rotterdam, P. Barts, E. Van Heusden, W. Burr, Models of neuronal populations: the basic mechanisms of rhythmicity, Progress in Brain Research 45 (1976) 281.
[16] F.H. Lopes da Silva, A. Hoeks, H. Smits, L.H. Zetterberg, Model of brain rhythmic activity, Biological Cybernetics 15 (1) (1974) 27–37.
[17] S. Neuenschwander, J. Martinerie, B. Renault, F.J. Varela, A dynamical analysis of oscillatory responses in the optic tectum, Cognitive Brain Research 1 (3) (1993) 175–181.
[18] E. Ott, Chaos in Dynamical Systems, Cambridge University Press, 2002.
[19] J.P. Pijn, J. Van Neerven, A. Noest, F.H. Lopes da Silva, Chaos or noise in EEG signals; dependence on state and brain site, Electroencephalography and Clinical Neurophysiology 79 (5) (1991) 371–381.
[20] J. Theiler, On the evidence for low-dimensional chaos in an epileptic electroencephalogram, Physics Letters A 196 (5–6) (1995) 335–341.
[21] Y. Wang, Z. Wang, J. Liang, On robust stability of stochastic genetic regulatory networks with time delays: a delay fractioning approach, IEEE Transactions on Systems, Man, and Cybernetics, Part B: Cybernetics 40 (3) (2010) 729–740.
[22] Z. Wang, X. Liu, Y. Liu, J. Liang, V. Vinciotti, An extended Kalman filtering approach to modeling nonlinear dynamic gene regulatory networks via short gene expression time series, IEEE/ACM Transactions on Computational Biology and Bioinformatics (TCBB) 6 (3) (2009) 410–419.
[23] F. Wendling, J.J. Bellanger, F. Bartolomei, P. Chauvel, Relevance of nonlinear lumped-parameter models in the analysis of depth-EEG epileptic signals, Biological Cybernetics 83 (4) (2000) 367–378.
[24] S. Wiggins, Introduction to Applied Nonlinear Dynamical Systems and Chaos, Springer Verlag, 2003.
[25] H.R. Wilson, J.D. Cowan, Excitatory and inhibitory interactions in localized populations of model neurons, Biophysical Journal 12 (1) (1972) 1–24.

Gan Huang got his Bachelor and Master degree form Department of Mathematics at Southeast University, China, in 2005 and 2008, respectively. Now he is a Ph.D. student in Shanghai Jiao Tong University, China. His research interests include BCI technology, EEG signal modeling, processing and classification.

Dingguo Zhang received the B.Eng. degree in electrical engineering from Jilin University and the M.Eng. degree in control engineering from Harbin Institute of Technology, China, in 2000 and 2002, respectively. He got the Ph.D. degree from Nanyang Technological University, Singapore, in 2007. From 2006 to 2007, he worked as a research fellow in Biorobtoics Lab of Nanyang Technological University, Singapore. In 2008, he was a postdoctoral fellow in LIRMM of CNRS, France. He is currently an Associate Professor in Institute of Robotics at Shanghai Jiao Tong University, China. His research interests include biorobotics, biomechatronics, biological cybernetics, and BCI/EMG technique.

Jianjun Meng got his Bachelor degree form School of Mechanical Engineering at Shanghai Jiao Tong University, China, in 2005. Now he is pursuing his Ph.D. degree. His research interest is focused on BCI technology, EEG signal processing.

Xiangyang Zhu obtained the B.S. degree from the Department of Automatic Control Engineering, Nanjing Institute of Technology, Nanjing, China, in 1985, the M.Phil. degree in instrumentation engineering from Southeast University, Nanjing, China, in 1989, and the Ph.D. degree in automatic control engineering from the same university in 1992. He joined the Department of Mechanical Engineering, Southeast University in 1995, after two years work as a postdoctoral fellow in Huazhong University of Science and Technology, Wuhan, China. Since June 2002, he has been a professor of Shanghai Jiao Tong University, with a joint appointment in the Robotics Institute and the State Key Laboratory of Mechanical Systems and Vibrations. His current research interests include robotic manipulation planning, manufacturing automation, and biomechatronics. Dr. Zhu was awarded the National Science Fund for Distinguished Young Scholars in 2005, and appointed as a Cheung Kong Chair Professor in 2007.